Water Incorporation

DOI: 10.1002/anie.200701765

Peculiar Nonmonotonic Water Incorporation in Oxides Detected by Local In Situ Optical Absorption Spectroscopy

Ji Haeng Yu, Jong-Sook Lee, and Joachim Maier**

High-temperature proton conductors are presumed to play an important role in the context of electrochemical energy conversion. This is due to their applicability in an intermediate temperature range that is high enough to enable fast kinetics and low enough to avoid many corrosion problems.[1] Typically, such materials are internally (partially) hydroxylated perovskite-structured oxides.[2–12] They are formed in the following way: the acceptor-doped oxides, which are rich in oxygen vacancies, absorb water such that oxygen vacancies are filled by hydroxide (OH^-) ions and the remaining H^+ ions are then attached to regular O^{2-} constituents. As a result of the dissociative incorporation of a single H_2O molecule, two internal hydroxide groups form at the cost of a single oxygen vacancy.[2]

In Equation (1), $V_O^{\bullet\bullet}$ and $OH_O^{\bullet}$ represent oxygen vacancies and hydroxide ions occupying oxygen sites, respectively. The dots indicate that the defect species are positively charged relative to the regular O^{2-} constituents (O_O).

$$H_2O + V_O^{\bullet\bullet} + O_O \rightleftharpoons 2\,OH_O^{\bullet} \qquad (1)$$

This incorporation generates significant proton conductivity in the solid state, the mechanism of which has been elucidated in the last two decades (see, for example, Refs. [12–14]). It is essentially a phonon-assisted proton transport that can be described by Equation (2).

$$OH^- + O^{2-} \rightarrow [O\cdots H\cdots O]^{3-} \rightarrow O^{2-} + OH^- \qquad (2)$$

The absorption mechanism consists of surface-reaction steps, during which water molecules are adsorbed, dissociated, and incorporated,[15] followed by a motion of protons and oxygen ions in the bulk phase. In the case where electronic conduction is negligible, the motion of H_2O in such crystals occurs as a coupled transport of $2\,H^+$ and O^{2-} ions[4,12] (Figure 1).

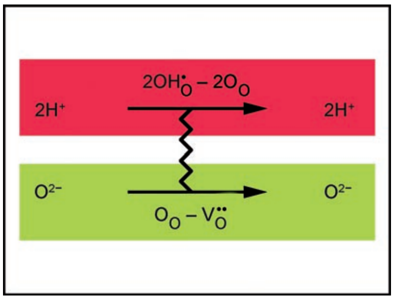

Figure 1. Water motion by coupled transport of $2\,H^+$ and O^{2-} ions. Proton motion occurs according to Equation (2), that is, by forming $OH_O^{\bullet}$ at the expense of O_O. Motion of the oxygen ions occurs by occupation of oxygen vacancies ($V_O^{\bullet\bullet}$) and formation of O_O.

Herein we report on the surprising nonmonotonic kinetics observed upon incorporation of water into an acceptor-doped oxide (Fe-doped $SrTiO_3$), which is unexpected in view of Figure 1. The results suggest, in simple terms, that in the presence of three carriers, the acid–base reaction [Eq. (3)] can

$$H_2O(g) \rightleftharpoons \text{“}H_2O\text{”}(SrTiO_3) \qquad (3)$$

be kinetically decomposed into two redox reactions: 1) hydrogenation, that is, reduction as a result of the fast ambipolar motion of H^+ ions and electronic carriers, and 2) oxygenation as a result of the sluggish motion of oxide ions together with electronic carriers (Figure 2). Powerful experimental tools permit the detailed understanding of water incorporation in terms of the temporal and spatial interplay of the two reactions.

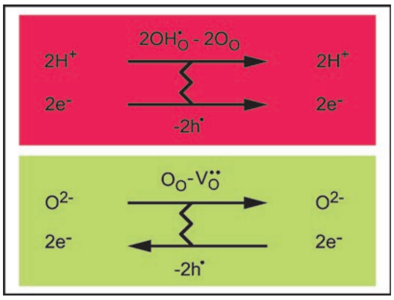

Figure 2. Motion of water by the decoupled transport of $2\,H^+$ and O^{2-} ions, with electroneutrality maintained by electronic carriers. The electronic flow occurs through a hole mechanism.

The incorporation of oxygen in oxides is usually monitored by either integral in situ methods—such as following the

---

[*] Prof. J.-S. Lee
School of Materials Science and Engineering
Chonnam National University
500-757 Gwangju (Korea)
Fax: (+82) 62-530-1699
E-mail: jongsook@jnu.ac.kr

Prof. J. Maier
Max Planck Institute for Solid State Research
Heisenbergstrasse 1, 70569 Stuttgart (Germany)
Fax: (+49) 711-689-1722
E-mail: s.weiglein@fkf.mpg.de

Dr. J. H. Yu
Korea Institute of Energy Research
305-343 Daejeon (Korea)

change in the overall conductance (see, for example, Refs. [16,17]) or weight over time after varying the oxygen partial pressure—or spatially resolving ex situ methods—such as the investigation of a frozen-in profile, for example, by secondary ion mass spectroscopy (SIMS; see, for example, Ref. [18]). In the current study we employed an optical absorption spectroscopic method that allows for an in situ detection of such redox reactions as a function of space and time at high temperatures. This method was developed by our research group[19] to study the incorporation of oxygen in $SrTiO_3$, and considers the local absorption as a function of the Fe^{4+}/Fe^{3+} ratio in the oxide, the value of which is an unambiguous measure of the local oxygen content.[19–22] As shown in Figure 3, the technique allows a precise detection of the kinetics not only in the diffusion-controlled case (a), but also in the cases in which the rate is controlled by the surface reaction (b) or even controlled by the transport through internal interfaces (c). For a clearer presentation, the images are presented in false colors that represent the local Fe^{4+}/Fe^{3+} ratio. In the first case (a) we observe diffusion profiles that develop in the expected way, in the second case (b) we observe homogeneous profiles that vary over time, and in the third case (c) we observe more or less homogeneous profiles in front of and behind the internal interface but which are separated by a step over the boundary. In all cases the transients are strictly monotonic.

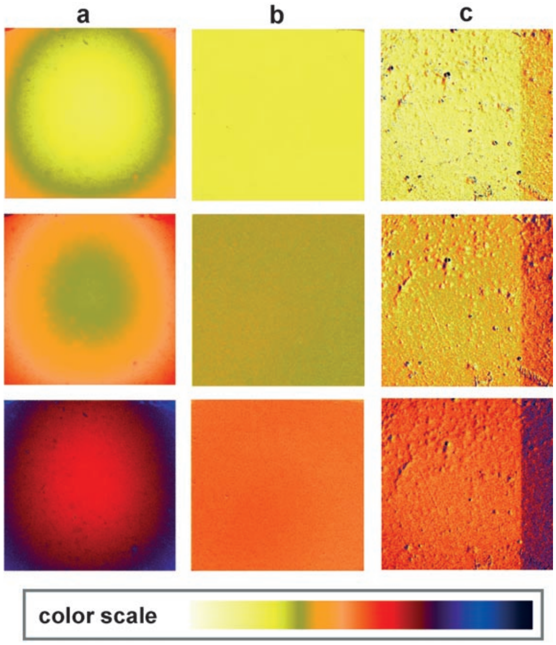

Figure 3. In situ optical absorption images of oxygen incorporation in Fe-$SrTiO_3$ through diffusion-controlled (a), surface-reaction controlled (b), or (blocking) grain boundary controlled processes (c).[19–21] The time sequence is from top to bottom after a stepwise increase in the oxygen partial pressure. At $t=0$ and $t=\infty$, the profiles are in accord with the colors given at the very left and the very right side of the scale which represents the increasing concentration of Fe^{4+} ions.

In the case of the incorporation of H_2O into $SrTiO_3$ we observe a highly peculiar feature that is shown in Figure 4.

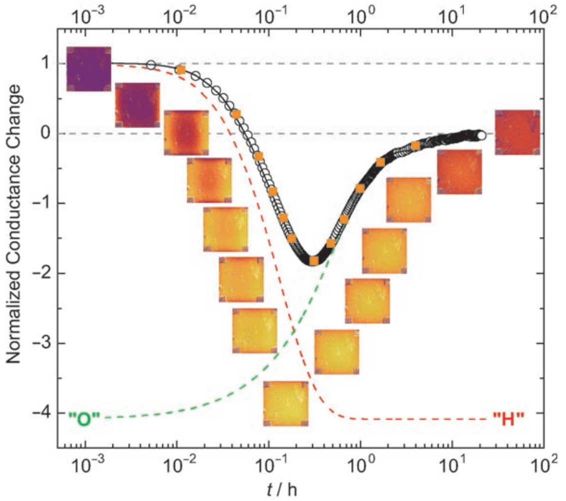

Figure 4. In situ optical absorption images of a $SrTiO_3$ single crystal ($6\times6\times1$ mm^3) doped with 5×10^{18} cm^{-3} Fe upon stepwise increase in the water vapor pressure from 4 mbar to 20 mbar in pure oxygen at 650 °C at times indicated by the squares on the conductance relaxation curve (in circles) of the same specimen. The left/right faces were coated with platinum, while the top/bottom remained bare and the large planar surfaces were sealed in glass. The conductance curve (cut-off at ca. 4 h) is described by the superposition of the hydrogenation (red) and oxidation (green) processes.

The Fe^{4+}/Fe^{3+} ratio of the final equilibrium state ($t=\infty$) is only slightly decreased from the value of the initial state ($t=0$), which is consistent with the defect-chemical calculation.[23] The transients, however, show severe redox changes. Clearly the sample is first strongly reduced and later oxidized. If there were only mobile H^+ and O^{2-} ions, an overshooting of the H^+ ions could only occur in the space–charge regions in which the electroneutrality condition does not apply.[24,25] The incorporation of H^+ and O^{2-} ions would necessarily be coupled in the case of bulk transport (Figure 1).[12] Since we have to consider three carriers, it is certainly conceivable that "H" penetrates first, thereby reducing the sample beyond the final equilibrium state, a situation that is ironed out by slowly penetrating "O". Electroneutrality can be maintained at all times in the bulk material as a consequence of the presence of electronic carriers. The strong non-equilibrium reduction can be quantitatively explained through a defect-chemical calculation[23] by assuming a "frozen" oxygen lattice with a constant concentration of the oxygen vacancies that corresponds to the initial state.

Optical absorption images recorded after short time periods reveal the pronounced color inhomogeneity in the horizontal profiles, which indicate a high catalytic activity for the incorporation of hydrogen at the platinum-coated surface (left/right sides). Slowly setting-in oxidation fronts can be seen by the orange tinges on the left and right edge of the images in the following sequences. The hydrogen-diffusion process in the bulk phase of the crystal appears spatially confined within these slowly moving oxidation fronts. The kinetics of the oxidation process beyond the overshooting point ($t > \approx 0.3$ h) is approximately comparable to that of oxygen incorporation shown in Figure 3.

Here it may suffice to state that the experimental conductance curve in Figure 4 can be described by a predominantly diffusion-controlled hydrogenation process ($D_{\mathrm{red}} = 8.2 \times 10^{-5}\,\mathrm{cm^2\,s^{-1}}$) and an oxygenation process apparently controlled both by diffusion and surface reaction ($D_{\mathrm{ox}} = 3.7 \times 10^{-5}\,\mathrm{cm^2\,s^{-1}}$ and $k_{\mathrm{ox}} = 2.9 \times 10^{-4}\,\mathrm{cm\,s^{-1}}$), which is in accord with the results obtained by optical spectroscopy. More details are beyond the scope of this report.

In summary, three issues have been highlighted: 1) the first spatially resolved in situ study of water incorporation by optical absorption spectroscopy; 2) the surprising appearance of nonmonotonic kinetics, which are rendered possible by the presence of more than two mobile carriers even though electroneutrality is maintained and the force-flux laws are assumed to be locally linear; 3) a mechanistic and quantitative explanation of the results by the decomposition of an acid–base process into two kinetically decoupled redox processes.

Received: April 20, 2007
Revised: August 26, 2007

Keywords: kinetics · optical absorption spectroscopy · oxides · protons · water

---

[1] J. Fleig, K. D. Kreuer, J. Maier, *Handbook of Advanced Ceramics*, *Vol. II*, Elsevier, Singapore, **2003**, pp. 59–105.
[2] S. M. Haile, *Mater. Today* **2003**, *6*, 24.
[3] S. Stotz, C. Wagner, *Ber. Bunsen-Ges.* **1966**, *70*, 781–788.
[4] R. Waser, *Ber. Bunsen-Ges.* **1986**, *90*, 1223–1230.
[5] H. Iwahara, T. Esaka, H. Uchida, N. Maeda, *Solid State Ionics* **1981**, *3–4*, 359–363.
[6] P. Murugaraj, K. D. Kreuer, T. He, T. Schober, *Solid State Ionics* **1997**, *98*, 1–6.
[7] D. G. Thomas, J. J. Lander, *J. Chem. Phys.* **1956**, *25*, 1136–1142.
[8] Y. Larring, T. Norby, *Solid State Ionics* **1995**, *77*, 147–151.
[9] A. S. Nowick, Y. Du, *Solid State Ionics* **1995**, *77*, 137–146.
[10] K.-D. Kreuer, *Chem. Mater.* **1996**, *8*, 610–641.
[11] T. Norby, M. Widerøe, R. Glöckner, Y. Larring, *Dalton Trans.* **2004**, 3012–3018.
[12] K. D. Kreuer, E. Schönherr, J. Maier, *Solid State Ionics* **1994**, *70–71*, 278–284.
[13] H. Iwahara, H. Uchida, K. Ono, K. Okaki, *J. Electrochem. Soc. J. Electrochem. Soc.* **1988**, *135*, 529–533.
[14] K. D. Kreuer, W. Münch, U. Traub, J. Maier, *Ber. Bunsen-Ges.* **1998**, *102*, 552–559.
[15] There are also oxides in which water is dissolved as a molecule ($NaCoO_2$).
[16] R. Metselaar, P. K. Larsen, *J. Phys. Chem. Solids* **1976**, *37*, 599–605.
[17] J. Maier, *Physical Chemistry of Ionic Materials. Ions and Electrons in Solids*, Wiley, Chichester, **2004**.
[18] R. A. De Souza, J. A. Kilner, C. Jeynes, *Solid State Ionics* **1997**, *97*, 409–419.
[19] I. Denk, F. Noll, J. Maier, *J. Am. Ceram. Soc.* **1997**, *80*, 279–285.
[20] M. Leonhardt, J. Jamnik, J. Maier, *Electrochem. Solid-State Lett.* **1999**, *2*, 333–335.
[21] M. Leonhardt, R. A. De Souza, J. Claus, J. Maier, *J. Electrochem. Soc.* **2002**, *149*, J19–J26.
[22] T. Bieger, J. Maier, R. Waser, *Ber. Bunsen-Ges.* **1993**, *97*, 1098–1104.
[23] J. H. Yu, J.-S. Lee, J. Maier, *Phys. Chem. Chem. Phys.* **2005**, *7*, 3560–3564.
[24] J. Jamnik, J. Maier, *Ber. Bunsen-Ges.* **1997**, *101*, 23–40.
[25] J. Jamnik, J. Maier, *J. Phys. Chem. Solids* **1998**, *59*, 1555–1569.